

Intermolecular Interactions in (Arene)chromium Carbonyl Compounds: Prediction of Chiral Crystal Packing from Racemate Structure

Susan E. Gibson (née Thomas),* Hasim Ibrahim, and Jonathan W. Steed*

Contribution from the Department of Chemistry, King's College London, Strand, London WC2R 2LS, U.K.

Received September 6, 2001

Abstract: Six X-ray crystal structures are reported, all containing substituted triphenylmethanol derivative **4** either alone or as its mono or bis(chromium tricarbonyl) complexes. All four chromium complexes studied crystallize with two independent molecules in the crystallographic asymmetric unit. It is demonstrated that from the X-ray crystal structure of the acentric racemic (\pm) - $(1pR,1''R)(1pS,1''S)$ -[Cr(CO)₃(η^6 -*t*-Bu-C₆H₃(CMeOMe)CPh₂OH)], (\pm) -**3**, it is possible to deduce the 4-fold helical structure of the chiral $(-)$ - $(1pR,1''R)$ isomer, $(-)$ -**3**. The bimetallic derivatives demonstrate the ability to control intermolecular interactions by the positioning of relative stereochemistry.

Introduction

Crystal engineering is a science that aims to both predict and control solid-state architecture: connectivity, mutual orientations, and symmetry.^{1–9} Successful crystal engineering has implications in the fabrication of nonlinear optical (NLO) materials (for which crystal polarity is a prerequisite), polymorph control, control of solid-state reactivity, and the design of composite materials.^{10–19} These goals have largely yet to be realized;²⁰ however, the identification and prediction of recognizable, recurring solid-state packing motifs are a reality.^{3,21} In cases where such motifs can be *isolated* from other interactions of importance, the reproducibility of these motifs, and hence

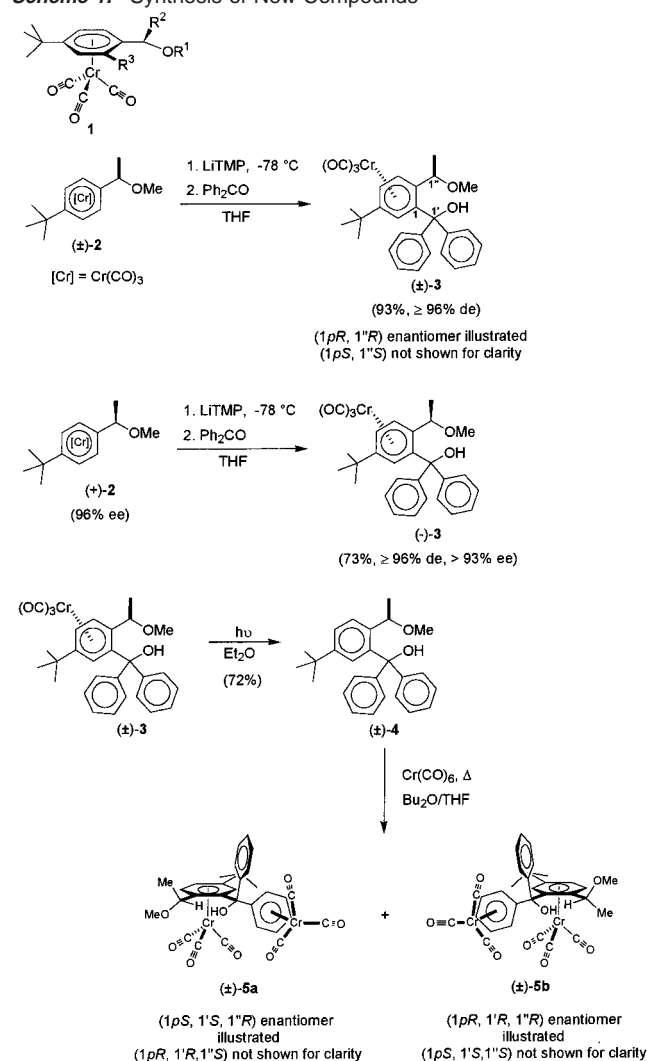
their predictive value, increases.^{5,9} Thus the predominance of the strongly hydrogen-bonded carboxylic acid dimer allows the design of numerous networks and topologies.²² Similarly, many general rules can be laid down about crystal packing within a wide variety of organic and metallo-organic systems.⁴ More specific generalizations may often be made as well, as demonstrated by Etter.²³ The introduction of polarity into solid-state systems is of particular interest in the design of NLO materials.²⁴ While this is generally possible to engineer given a chiral molecule (resolved chiral compounds must crystallize in polar space groups in the absence of disorder), it is of much greater economy to be able to engineer polar and/or chiral solid-state structures from achiral or racemic building blocks. The occurrence of bulk crystal chirality (and its spontaneous resolution) in the absence of molecular chirality is much more haphazard, however, and often limited to very specific compounds.

Recently one of us has demonstrated the occurrence of crystal chirality arising from helix formation as a result of weak CH \cdots O=P interactions irrespective of the handedness of one of two chiral centers in the phosphonate building block.²⁵ We have also recently carried out studies on nonglass solid-state structures with a large number of crystallographically independent molecules (i.e., $Z' > 1$)^{26,27} with a view to introducing “designer asymmetry”.^{14,28–30} Independently, two of us have developed a preparative route that allows the efficient enantio- and

- (1) Desiraju, G. *Angew. Chem., Int. Ed. Engl.* **1995**, *34*, 2311.
- (2) Braga, D.; Maini, L.; Grepioni, F. *Angew. Chem., Int. Ed.* **1998**, *37*, 2240–2242.
- (3) Thalladi, V. R.; Goud, B. S.; Hoy, V. J.; Allen, F. H.; Howard, J. A. K.; Desiraju, G. R. *Chem. Commun.* **1996**, 401–402.
- (4) Braga, D.; Grepioni, F.; Desiraju, G. R. *Chem. Rev.* **1998**, *98*, 1375.
- (5) Desiraju, G. R. In *The Crystal As a Supramolecular Entity*; Lehn, J. M., Ed.; John Wiley & Sons: Chichester, 1996; Vol. 2.
- (6) Desiraju, G. R. *The Design of Organic Solids*; Elsevier: Amsterdam, 1989.
- (7) Burrows, A. D.; Harrington, R. W.; Mahon, M. F.; Price, C. E. *J. Chem. Soc., Dalton Trans.* **2000**, 3845–3854.
- (8) Guliera, G.; Steed, J. W. *Chem. Commun.* **1999**, 1563–1564.
- (9) Desiraju, G. R.; Steiner, T. *The Weak Hydrogen Bond*; OUP/IUPAC: Oxford, 1999.
- (10) Sarma, J. A. R. P.; Allen, F. H.; Hoy, V. J.; Howard, J. A. K.; Thaimattam, R.; Biradha, K.; Desiraju, G. R. *Chem. Commun.* **1997**, 101–102.
- (11) Zaworotko, M. J. *Chem. Soc. Rev.* **1994**, *23*, 283.
- (12) Thalladi, V. R.; Boese, R.; Brasselet, S.; Ledoux, I.; Zyss, J.; Jetti, R. K. R.; Desiraju, G. R. *Chem. Commun.* **1999**, 1639–1640.
- (13) Steed, J. W.; Atwood, J. L. *Supramolecular Chemistry: An Introduction*; J. Wiley & Sons: Chichester, 2000.
- (14) Prince, P. D.; McGrady, G. S.; Steed, J. W. *New J. Chem.* **2001**, in press.
- (15) Dunitz, J. D.; Fillippini, G.; Gavezzotti, A. *Helv. Chim. Acta* **2000**, *83*, 2317–2335.
- (16) Anwar, J. J. *Pharm. Pharmacol.* **1998**, *50*, 51.
- (17) Kordikowski, A.; Shekunov, T.; York, P. *Pharm. Res.* **2001**, *18*, 682–688.
- (18) Schmidt, G. M. J. *J. Chem. Soc.* **1964**, 2014.
- (19) Nichols, P. J.; Raston, C. L.; Steed, J. W. *Chem. Commun.* **2001**, 1062–1063.
- (20) Gavezzotti, A. *Acc. Chem. Res.* **1994**, *27*, 309–314.
- (21) Allen, F. H.; Howard, J. A. K.; Hoy, V. J.; Desiraju, G. R.; Reddy, D. S.; Wilson, C. C. *J. Am. Chem. Soc.* **1996**, *118*, 4081.

- (22) Atwood, J. L.; Davies, J. E. D.; MacNicol, D. D.; Vögtle, F. *Comprehensive Supramolecular Chemistry*, 1st ed.; Pergamon: Oxford, 1996; Vol. 6.
- (23) Etter, M. C. *Acc. Chem. Res.* **1990**, *23*, 120–126.
- (24) Marder, S. R. *Metal Containing Materials for Nonlinear Optics*, 2nd ed.; Wiley: Chichester, 1996; pp 121–169.
- (25) Forristal, I.; Lowman, J.; Afarinkia, K.; Steed, J. W. *CrystEngComm* **2002**, *2*, 457–461.
- (26) Steiner, T. *Acta Crystallogr., Sect. B* **2000**, *56*, 673–676.
- (27) Brock, C. P. *J. Res. Natl. Inst. Stand. Technol.* **1996**, *101*, 321–325.
- (28) Hassaballa, H.; Steed, J. W.; Junk, P. C.; Elsegood, M. R. *J. Inorg. Chem.* **1998**, *37*, 4666–4671.
- (29) Steed, J. W.; Hassaballa, H.; Junk, P. C. *Chem. Commun.* **1998**, 577–578.
- (30) Steed, J. W.; Sakellariou, E.; Junk, P. C.; Smith, M. *Chem.-Eur. J.* **2001**, *7*, 1240–1247.

Scheme 1. Synthesis of New Compounds



diastereoselective synthesis of a wide range of arene tricarbo-nylchromium(0) complexes of type **1**.^{31,32} We now report a unique study in crystal engineering that brings together highly stereoselective molecular and crystal synthesis allowing the preparation and control of a range of resolved, chiral solid-state compounds with $Z' > 1$.

Results and Discussion

Treatment of the sterically hindered racemic arene tricarbo-nylchromium(0) (\pm)-**2** with LiTMP (lithium tetramethylpiperidine) at -78°C followed by quenching with 3 equiv of benzophenone leads to clean ortho-substitution to give the racemic monoalcohol (\pm)-**3** in 93% yield and over 96% diastereomeric excess, Scheme 1. This efficient diastereoselectivity is the result of the preferred conformation in the lithiated intermediate which minimizes steric interactions between the benzylic group and the $\text{Cr}(\text{CO})_3$ fragment.³³ The analogous reaction with (+)-**2**, generated using chiral base methodology,³¹ affords almost enantiomerically pure ($-$)-**3** ($> 96\%$ de, $> 93\%$ ee).

The X-ray crystal structure of (\pm)-**3** exhibits two crystallographically independent molecules ($Z' = 2$, see Table 1 for crystallographic data for new compounds). Intriguingly, the two molecules in the asymmetric unit are enantiomers ($1pR, 1'R$ and $1pS, 1'S$), and yet they do not give rise to a centrosymmetric structure. In fact, the compound crystallizes in the noncentrosymmetric but achiral space group $Pna2_1$. Bond lengths and angles within the two independent molecules are within normal bounds and will not be discussed further. Consistent with Etter's rules,²³ it would be anticipated that the crystal packing would be dominated by hydrogen bonds involving the hydroxyl functionality, and indeed this proves to be the case. Starting with molecule **1**, based on Cr(1) (an SS enantiomer), the OH group interacts with the strongest hydrogen bond acceptor, the OMe functionality ($\text{O}(2)\cdots\text{O}(6)$), on the adjacent, independent RR enantiomer, molecule **2**, within the same asymmetric unit. Molecule **2**, in turn, hydrogen bonds to the OMe group on a further RR enantiomer ($\text{O}(7)\cdots\text{O}(1')$, generated from molecule **1** by glide symmetry). This RR enantiomer then interacts via an $\text{O}(2)\cdots\text{O}(6)$ hydrogen bond to an SS enantiomer generated from molecule **2**. The result is an infinite hydrogen-bonded chain comprising the following sequence: $SS\cdots RR\cdots RR\cdots SS\cdots SS\cdots RR\cdots$ etc., that is, alternating homochiral and heterochiral pairings. The angle between the heterochiral pair (hydrogen bond $\text{O}(2)\cdots\text{O}(6)$) is ca. 30° (Figure 1a), whereas between the homochiral pair the second independent hydrogen bond induces a twist of ca. 90° , approximating to a 4_1 screw operation (Figure 1b). Interestingly, when the homochiral pair is subjected to the crystallographic 2_1 screw operation that forms part of the space group symmetry, the result is a 4-fold helix with pitch 15.28 Å. The helix comprises four molecules all of the same handedness, held together by alternating homochiral hydrogen bonds and edge-to-face π -stacking interactions, Figure 2.

Racemic (\pm)-**3** cocrystallizes with two molecules of dichloromethane. As the next strongest hydrogen bond donors, the CH protons of the CH_2Cl_2 molecules interact with the next strongest hydrogen bond acceptors, the CO ligands, and fulfill a space-filling role.

The structure of (\pm)-**3** is extremely interesting from a crystal engineering viewpoint because it gives significant insight into the interactions between pairs of identical enantiomers without the need to prepare the enantiomerically pure material. This enables us to make confident predictions about the structure of a resolved enantiomer of **3**, viz ($-$)-**3**. In the absence of the opposite enantiomer, *only* homochiral pairings will result, giving a hydrogen-bonded chain of type $RR\cdots RR\cdots RR\cdots RR\cdots$. This pairing arises from a crystallographic glide operation in (\pm)-**3**, but, in a resolved material, it is not possible for the compound to crystallize in an achiral space group (i.e., inversion, mirror, and glide operations are ruled out). Thus, to maintain the same homochiral hydrogen-bonded interaction in ($-$)-**3** as observed in (\pm)-**3** there must *necessarily* be two independent molecules of the same chirality ($Z' = 2$). Note that while Z' is also equal to 2 in (\pm)-**3** this is for an entirely different reason, the presence of two independent types of hydrogen bond (homochiral and heterochiral). If we subtract glide operations from the achiral space group of (\pm)-**3** ($Pna2_1$), we are left with the chiral space group $P2_1$. Thus, a possible structure for ($-$)-**3** (or its enantiomer) would be a 4-fold hydrogen-bonded helix comprising two

(31) Cowton, E. L. M.; Gibson (née Thomas), S. E.; Schneider, M. J.; Smith, M. H. *Chem. Commun.* **1996**, 839–840.

(32) Ibrahim, H.; Gibson, S. E. *Chem. Commun.* **2001**, 1070–1071.

(33) Heppert, J. A.; Aubé, J.; Thomas-Miller, M. E.; Milligan, M. L.; Takusagawa, F. *Organometallics* **1990**, 9, 727.

Table 1. Crystallographic Data for New Compounds

	(±)- 4	(±)- 4 ·Me ₂ CO	(±)- 3 ·2CH ₂ Cl ₂	(-)- 3 ·2CH ₂ Cl ₂	(±)- 5a	(±)- 5b ·CH ₂ Cl ₂
formula	C ₂₆ H ₃₀ O ₂	C ₂₉ H ₃₆ O ₃	C ₃₀ H ₃₂ Cl ₂ CrO ₅	C ₃₀ H ₃₂ Cl ₂ CrO ₅	C ₃₂ H ₃₀ Cr ₂ O ₈	C _{32.5} H ₃₁ ClCr ₂ O ₈
formula weight (g mol ⁻¹)	374.5	432.58	595.46	595.46	646.56	689.02
temperature (°C)	-153(2)	-153(2)	-173(2)	-153(2)	-153(2)	-153(2)
wavelength (Å)	0.71073	0.71073	0.71073	0.71073	0.71073	0.71073
space group	<i>P</i> 2 ₁ 2 ₁ 2 ₁	<i>P</i> 2 ₁	<i>Pna</i> 2 ₁	<i>P</i> 4 ₁	<i>P</i> 2 ₁ 2 ₁ 2 ₁	<i>P</i> 1
unit cell dimensions (Å, deg)						
<i>a</i>	10.0416(8)	8.6518(6)	27.4425(6)	19.7635(6)	10.4305(4)	12.7753(6)
<i>b</i>	11.4518(8)	10.0312(8)	13.8076(2)	19.7635(6)	18.1260(8)	13.2878(6)
<i>c</i>	18.8534(9)	14.6724(9)	15.2781(4)	15.1720(7)	30.9046(11)	18.6941(8)
α						77.804(3)
β		97.809(4)				89.098(3)
γ						89.761(2)
volume (Å ³)	2168.0(3)	1261.58(15)	5789.1(2)	5926.1(4)	5842.9(4)	3101.4(2)
<i>Z</i>	4	2	8	8	8	4
<i>D</i> _c (g cm ⁻³)	1.147	1.139	1.366	1.335	1.470	1.476
μ (mm ⁻¹)	0.071	0.072	0.617	0.603	0.795	0.837
<i>F</i> (000)	808	468	2480	2480	2672	1420
θ range (deg)	2.9–26.0	2.6–26.0	2.7–26.0	2.7–26.0	2.1–27.5	1.6–26.0
reflections collected	12 448	6995	27 315	36 245	21 498	18 869
independent reflections	4250	4276	10 486	11 437	12 750	12 120
parameters	257	285	696	696	776	792
GOF on <i>F</i> ²	1.044	1.059	1.041	1.018	1.010	1.034
final <i>R</i> indices, <i>I</i> > 2 σ (<i>I</i>)	<i>R</i> 1 = 0.0680, w <i>R</i> 2 = 0.1446	<i>R</i> 1 = 0.0680, w <i>R</i> 2 = 0.1639	<i>R</i> 1 = 0.0598, w <i>R</i> 2 = 0.1031	<i>R</i> 1 = 0.0663, w <i>R</i> 2 = 0.1296	<i>R</i> 1 = 0.0494, w <i>R</i> 2 = 0.1190	<i>R</i> 1 = 0.0773, w <i>R</i> 2 = 0.1775
<i>R</i> indices (all data)	<i>R</i> 1 = 0.1144, w <i>R</i> 2 = 0.1640	<i>R</i> 1 = 0.0775, w <i>R</i> 2 = 0.1721	<i>R</i> 1 = 0.0908, w <i>R</i> 2 = 0.1131	<i>R</i> 1 = 0.1224, w <i>R</i> 2 = 0.1495	<i>R</i> 1 = 0.0667, w <i>R</i> 2 = 0.1285	<i>R</i> 1 = 0.1145, w <i>R</i> 2 = 0.1975
absolute structure parameter	0(3)	-1(2)	-0.01(2)	-0.04(2)	0.480(18)	
largest diff peak (e Å ⁻³)	0.457	0.525	0.899	0.538	0.999	1.188

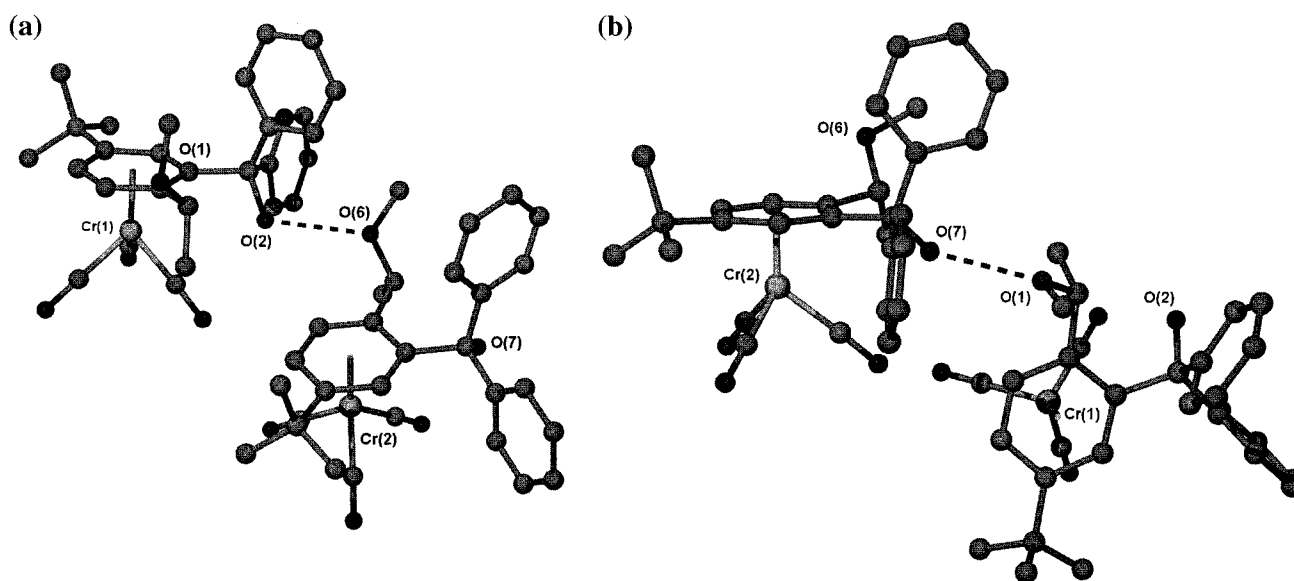


Figure 1. (a) The two independent chromium complexes in the asymmetric unit of (±)-**3**·2CH₂Cl₂ showing the heterochiral *SS'*···*RR* hydrogen bond, O(2)···O(6) 2.806(4) Å. (b) The crystallographically independent homochiral *RR*···*RR* hydrogen bond in (±)-**3**·2CH₂Cl₂, O(7)···O(1)' 2.721(4) Å (primed atom generated by glide operation $-x + 1/2, y - 1/2, z - 1/2$). Both unique pairings are supported by CH···OC interactions from the coordinated aryl rings to adjacent carbonyl ligands, with C···O distances in the range 3.177–3.331 Å.

pairs of crystallographically independent molecules (both *RR* so all interactions along the helical chain are homochiral), related by a crystallographic 2₁ axis.

While this is *necessarily* the only way to go from the observed homochiral interactions in (±)-**3** to a resolved structure containing only homochiral interactions, it is only part of the story, however. We have not yet accounted for the edge-to-face π - π

interactions which occur along the 2₁ axis in (±)-**3** (Figure 2). In (±)-**3** the π - π interaction is also homochiral and also results in a noncrystallographic 4₁ operation (noncrystallographic because it is between two crystallographically independent molecules). Thus, both *RR*···*RR* hydrogen bonding and *RR*···*RR* π - π interactions must result in 4-fold helix formation in the resolved material, leading to a predicted space group of *P*4₁.

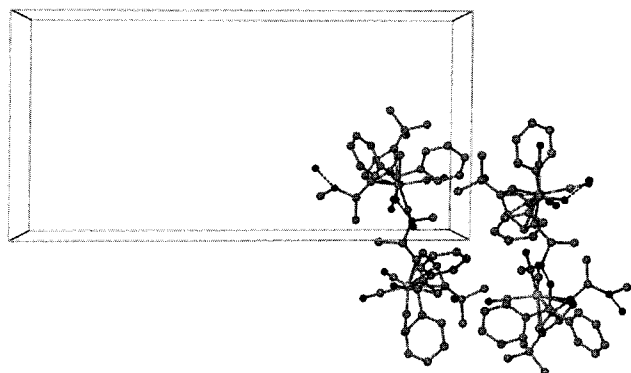


Figure 2. View down the crystallographic 2_1 axis (c axis, 15.2781(4) Å) showing the 4-fold helix resulting from the action of the 2_1 screw on the approximate 4_1 symmetry of the $RR\cdots RR$ pairing. Molecules related by 2_1 symmetry interact via edge-to-face π -stacking interactions.

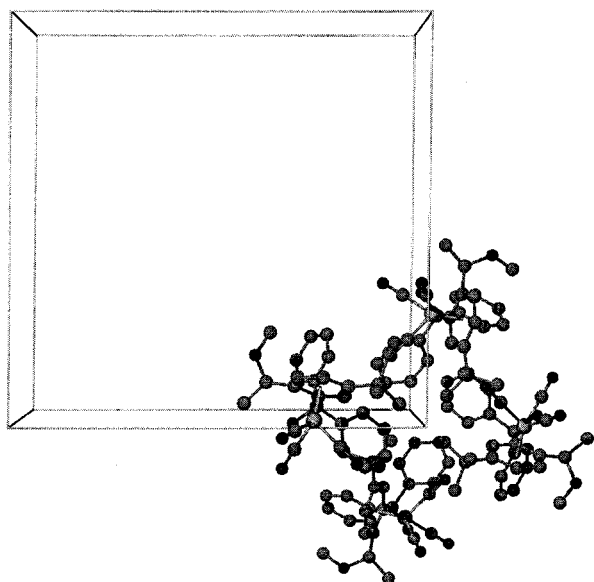


Figure 3. The crystallographic 4_1 helix in $(-)$ -**3** (c axis, 15.1720(7) Å). Interactions are entirely of the edge-to-face π - π type.

The same is, of course, true for the SS enantiomer. Conversely, the unobserved RS/SR diastereoisomer will have a significantly different packing mode.

The predictions derived from (\pm) -**3** were experimentally verified by the preparation of optically pure $(-)$ -**3** as detailed above. It proved extremely gratifying to find that $(-)$ -**3** does indeed crystallize in the chiral tetragonal space group $P4_1$ with $Z' = 2$. In the structure there are two independent 4-fold helices. One is situated on the crystallographic 4_1 axis in which the molecules interact entirely by edge-to-face π - π interactions (Figure 3). This results in a crystallographic c dimension very similar to that found along the 2_1 axis in (\pm) -**3** (Table 1). The other 4-fold helix results entirely from $\text{OH}\cdots\text{OME}$ hydrogen bonding interactions, identical to the homochiral interactions found in the racemate. The two independent hydrogen-bonded distances are very similar to the homochiral $RR\cdots RR$ combination found in (\pm) -**3**, but distinct from the longer $RR\cdots SS$ interaction. This helix is situated on a crystallographic 2_1 axis and involves two pairs of two unique $RR\cdots RR$ molecules, Figure 4.

Strident attempts were also made to prepare racemic and resolved samples of the opposite diastereoisomer of **3**, (\pm) - $(1pR,1''S)(1pS,1''R)$ - $[\text{Cr}(\text{CO})_5(\eta^6-t\text{-BuC}_6\text{H}_3(\text{CMeOMe})\text{CPh}_2-$

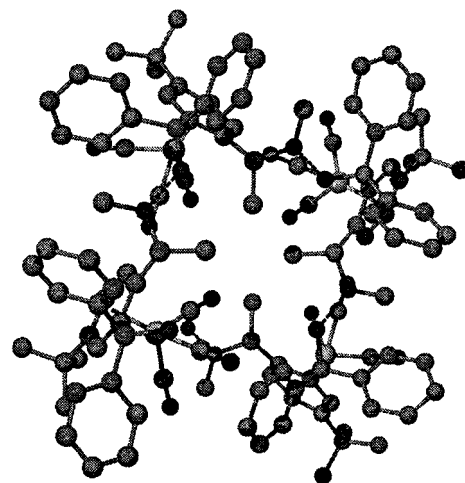


Figure 4. The noncrystallographic 4-fold helix in $(-)$ -**3**. Intermolecular hydrogen-bonded distances: $\text{O}(2)\cdots\text{O}(6)$ 2.732(5), $\text{O}(7)\cdots\text{O}(1')$ 2.726(5) Å (primed atom generated by 2_1 operation $2 - x, 1 - y, 1/2 + z$). Note that both distances are similar to the $\text{O}(7)\cdots\text{O}(1')$ distance in (\pm) -**3** but distinct from the heterochiral $\text{O}(2)\cdots\text{O}(6)$ hydrogen bond.

$\text{OH}]$, by protection of one of the ortho sites using SiMe_3 . The deprotonation reaction of the silylated material proved to be relatively difficult, however, and the attempt was abandoned.

The predictability of the structure of $(-)$ -**3** is predicated upon the isolation of the $\text{OH}\cdots\text{OME}$ interaction in particular as the dominant crystal packing driving force. To verify whether this was indeed the case, it was deemed of interest to also examine the X-ray structure of the free ligand (\pm) -**4**. The free substituted triphenylmethanol derivative (\pm) -**4** can be isolated in 72% yield by decomplexation of racemic (\pm) -**3** by irradiation with a 100 W light bulb over 7 days. Crystallization of **4** from a mixed acetone/ $\text{CH}_2\text{Cl}_2/n$ -pentane solution unfortunately results in the formation of a solvate $\mathbf{4}\cdot\text{OCMe}_2$ in which the hydroxyl functionality of the ligand interacts with the acetone carbonyl oxygen atom ($\text{OH}\cdots\text{O}$ 2.826(4) Å). However, crystallization from n -pentane affords the solvent free material, which does indeed display the expected $\text{OH}\cdots\text{OME}$ hydrogen bond, Figure 5. Remarkably both (\pm) -**4** and (\pm) - $\mathbf{4}\cdot\text{OCMe}_2$ crystallize in chiral space groups ($P2_12_12_1$ and $P2_1$, respectively) despite being present in solution in racemic form. Furthermore, both crystal structures are disordered and contain varying proportions of both enantiomers (83% of one enantiomer for (\pm) -**4** and 63% for (\pm) - $\mathbf{4}\cdot\text{OCMe}_2$; using molybdenum radiation it was not possible to determine whether the R or S form predominates). In the case of (\pm) - $\mathbf{4}\cdot\text{OCMe}_2$, this disorder has essentially no effect on the crystal packing since it involves two alternate positions for just two atoms near the chiral center (plus associated t -butyl group disorder). In solvent free (\pm) -**4**, however, the OME acceptor atom is disordered, and in the *minor* enantiomer (disordered component) it forms the shorter hydrogen bond with the nondisordered OH group of an adjacent molecule, $\text{O}\cdots\text{O}$ distances 2.685(5) versus 2.900(4) Å. The structures of (\pm) -**4** and its acetone solvate clearly establish that the OH group does indeed dominate the crystal packing and also highlight the awkward shape of the ligand, resulting in a high propensity for acentric crystal packing modes.

Reaction of (\pm) -**4** with 1 equiv of $\text{Cr}(\text{CO})_6$ results in a complicated mixture of products from which the bimetallic

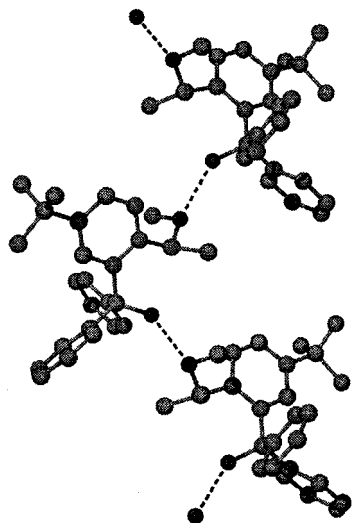


Figure 5. Twofold helical packing in (\pm)-**4** (solvent free) showing the hydrogen-bonded chain to the major component. Hydrogen bonds to the minor component are of the same form but shorter; OH \cdots O distances 2.685(5) and 2.900(4) Å.

complexes **5** may be isolated by column chromatography. Complexes **5** possess three chiral elements (two centers and plane chirality associated with the side of the trisubstituted aryl ring complexed to chromium). The compound can, theoretically, exist as a total of eight isomers comprising four diastereomeric pairs denoted (\pm)-(1*pR*,1'*R*,1''*R*)-**5**, (\pm)-(1*pR*,1'*R*,1''*S*)-**5**, (\pm)-(1*pR*,1'*S*,1''*S*)-**5**, and (\pm)-(1*pR*,1'*S*,1''*R*)-**5** (and their enantiomers). In practice, only (\pm)-(1*pR*,1'*R*,1''*S*)(1*pS*,1'*S*,1''*R*)-**5**, (\pm)-**5a**, and (\pm)-(1*pR*,1'*R*,1''*R*)(1*pS*,1'*S*,1''*S*)-**5**, (\pm)-**5b**, are observed and isolated (as racemates) from the reaction mixture.

The X-ray crystal structures of diastereoisomers **5a** and **5b** were determined, and both showed one Cr(CO)₃ unit to reside on the *tert*-butyl substituted ring (as in complexes **3**), while the second is coordinated to one of the phenyl substituents, rendering the -C*Ph₂OH central carbon atoms chiral. Remarkably, as for **3**, both structures displayed $Z' = 2$ with the two independent molecules being enantiomers of one another. (\pm)-**5b** also cocrystallizes with one disordered molecule of CH₂-Cl₂. The view down the HO-C* axis shows both Cr(CO)₃ groups to be pointing "up" toward the hydroxyl group in all four unique molecules in the two structures, consistent with steric arguments. While both structures contain two unique enantiomers, their crystal packing modes are distinctly different from one another. (\pm)-**5a** crystallizes in the chiral space group $P2_12_12_1$ and spontaneously resolves. Thus, while the crystal contains two enantiomers, it is chiral by virtue of the 2-fold helical crystal packing arrangement. In contrast, (\pm)-**5b** crystallizes in the centrosymmetric space group $P\bar{1}$, and thus each crystallographically independent enantiomer is related by inversion symmetry to a molecule of the opposite handedness. However, the two independent enantiomers are not symmetry-related to one another.

The chiral (\pm)-**5a** shows two distinctly different types of OH \cdots O hydrogen bond in the two independent molecules. The *SSR* enantiomer (containing atoms Cr(1) and Cr(2)) exhibits a homochiral intermolecular OH \cdots OC bond to one of the carbonyl ligands (not OMe group, cf. **3**) on an adjacent *SSR* enantiomer (Figure 6) to give an infinite crystallographic 2₁ helix along the *a* direction. The long O \cdots O distance of 2.946(4) Å is

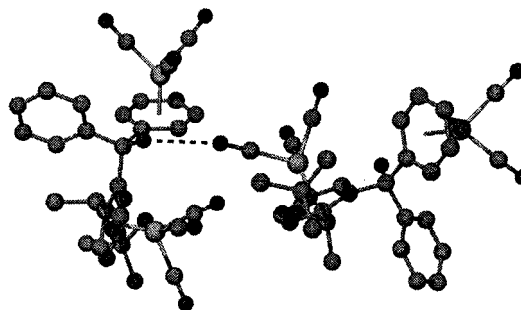


Figure 6. Intermolecular hydrogen bonding to CO in (\pm)-**5a** between two *RSS* enantiomers. Hydrogen-bonded distance 2.946(4) Å.

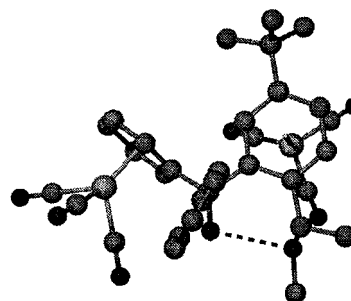


Figure 7. Intramolecular hydrogen bonding in (\pm)-**5a** by the *RSS* enantiomer. Hydrogen-bonded distance 2.659(4) Å.

consistent with the weak hydrogen bond acceptor nature of the CO ligand.³⁴ This is particularly surprising given the propensity in **3** for hydrogen bonding to the OMe group which should be a stronger acceptor and suggests that the bimetallic species is particularly sterically demanding. The independent *RSS* enantiomer, on the other hand, contains an *intramolecular* OH \cdots OMe interaction with the much shorter O \cdots O distance of 2.659(4) Å, Figure 7. This is also a surprising interaction given the purely intermolecular nature of the hydrogen bonds observed for compounds **3** and **4**. Furthermore, it seems only to be associated with the occurrence of opposite *R/S* handedness at the first chiral carbon atoms and the plane chiral element. This places the OMe group and OH group in close proximity. In contrast, in *RR* and *SS*-**3** they are orientated away from one another. Similarly, the other diastereoisomer (\pm)-**5b** shows only intermolecular OH \cdots OC hydrogen bonds. From this observation, we can therefore predict that the unobserved *RS*-**3** should show similar *intramolecular* hydrogen bonding.

Unlike its diastereoisomer, the two independent enantiomeric molecules in (\pm)-**5b** are directly hydrogen bonded together via entirely heterochiral OH \cdots OC interactions to form an infinite chain, Figure 8, with repeat *RRR* \cdots *SSS* \cdots *RRR* \cdots *SSS* \cdots . Interactions between the two independent molecules in (\pm)-**5a** are of the edge-to-face π - π type observed in **3**.

Conclusion

All compounds of type **3**–**5** are highly substituted monoalcohols, a class of compound known to commonly form structures with $Z' > 1$ (40% of monoalcohols have $Z' > 1$, as compared with 8.3% of the Cambridge Structural Database^{35,36} (CSD) as a whole^{27,37,38}). It is likely that this behavior is a result

(34) Braga, D.; Grepioni, F. *Acc. Chem. Res.* **1997**, *30*, 81–87.

(35) Fletcher, D. A.; McMeeking, R. F.; Parkin, D. *J. Chem. Inf. Comput. Sci.* **1996**, *36*, 746.

(36) Allen, F. H.; Kennard, O. *Chemical Design Automation News* **1993**, *8*, 31.

(37) Wilson, A. J. C. *Acta Crystallogr., Sect. A* **1993**, *49*, 795–806.

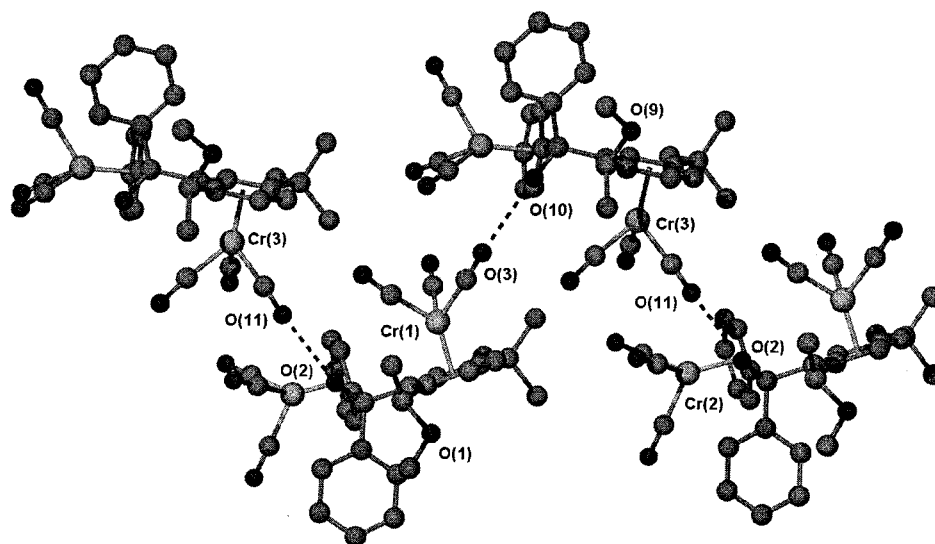


Figure 8. Infinite OH...OC hydrogen-bonded chain in (\pm)-**5b** comprising two independent heterochiral interactions. Hydrogen-bonded distances: O(10)...O(3)' 2.840(7), O(2)...O(11) 2.762(7) Å (primed atom generated by translation $x - 1, y, z$).

of the fact that the hydrogen bonding requirements of the OH group dominate the crystal packing, often resulting in frustration^{28–30} between the conflicting needs to achieve close packing and maximize hydrogen bonding to the lone OH group. Moreover, compounds **3–5** are all derivatives of triphenylmethanol. Triphenylmethanol along with its silicon and germanium analogues exhibits *eight* crystallographically independent molecules ($Z' = 8$). This is a consequence of the formation of two independent sets of hydrogen-bonded tetramers. Even in the absence of the OH group we have shown that compounds of type $YXPh_3$ ($Y = \text{halogen}$, $X = \text{group 14 element}$) exhibit an extremely high incidence of $Z' > 1$ as a consequence of weak aryl $CH\cdots Y$ interactions.¹⁴

In the particular case of ($-$)-**3** we have shown that it is possible to predict the precise nature of the crystal packing geometry by consideration of the structure of the analogous $Z' = 2$ racemate, which fortuitously crystallizes in an acentric space group and demonstrates homochiral interactions. We have also demonstrated that relative stereochemistry may be used to switch on and off particular intermolecular and intramolecular interactions. Furthermore, the sterically demanding nature of the system limits the number of possible intermolecular interactions, resulting in a high degree of reproducibility across many structures.

By extending this approach, it should be possible to make concrete predictions about the crystal packing mode of all resolved compounds for which the racemate crystallizes in such a way as to demonstrate the nature of homochiral interactions, assuming those interactions to be isolated and dominant. Furthermore, in selected cases, we can also use chirality to predict and engineer the incidence of structures with $Z' > 1$ (in the absence of disorder). Thus, a racemate displaying a centrosymmetric intermolecular interaction (e.g., formation of a carboxylic acid dimer) must double Z' upon resolution; that is, a resolved chiral mono carboxylic acid dimer must exhibit $Z' = 2$ if the racemate exhibits $Z' = 1$ with the two enantiomers related by inversion symmetry.

Experimental Section

Instrumental. All reactions and manipulations involving organometallic compounds were performed under an inert atmosphere of dry nitrogen, using standard vacuum line and Schlenk tube techniques. Reactions and operations involving (arene)tricarbonylchromium(0) complexes were protected from light. THF was distilled from sodium benzophenone ketyl. The concentration of methylolithium was determined by titration against diphenylacetic acid in THF. Tetramethylpiperidine was stored over potassium hydroxide. Flash column chromatography was performed using Merck silica gel 60 (230–400 mesh). All other reagents were used as obtained from commercial sources. Melting points were recorded in open capillaries on a Büchi 510 melting point apparatus and are uncorrected. IR spectra were recorded on Perkin-Elmer 1600 FT-IR. NMR spectra were recorded at room temperature on a Bruker AM 360 and DRX 400, and J values are reported in hertz. Mass spectra were recorded on a JEOL AX 505W and Kratos MS890MS. Elemental analyses were performed by the University of North London microanalytical service.

Preparations. (\pm)-(*1pR, 1''R*)(*1pS, 1''S*)- η^6 -[2-(1-Methoxyethyl)-5-*tert*-butyl-(diphenylhydroxymethyl) benzene]tricarbonylchromium-(**0**), (\pm)-**3**. Methylolithium (1.31 mL of a 1.76 M solution in diethyl ether, 2.3 mmol) was added dropwise at -78°C to a stirred solution of tetramethylpiperidine (0.39 mL, 2.3 mmol) in THF (20 mL). The solution was allowed to reach room temperature and recooled to -78°C . Complex (\pm)-**2** (657 mg, 2 mmol) in THF (8 mL) was added via a cannula, and the resulting orange solution was stirred for 1 h. A solution of benzophenone (1.26 g, 6.9 mmol) in THF (5 mL) was added via a cannula, and stirring was continued for a further 2 h at -78°C . The reaction vessel was removed from the acetone–dry ice bath, and the reaction mixture was stirred at room temperature for 1 h. Methanol was added, and the solvent was removed in vacuo. Flash column chromatography (SiO_2 ; hexane/diethyl ether, 10:0–5:5) of the residue gave the complex (\pm)-**3** as a yellow solid (950 mg, 93%). mp: 158 – 159°C . IR (Nujol, cm^{-1}): ν_{OH} 3386 (w), ν_{CO} 1953 (s), 1946 (m), 1879 (m), 1868 (s), 1860 (s). ^1H NMR (360 MHz, CDCl_3): δ 1.09 (s, 9H, $(\text{CH}_3)_3\text{C}$), 1.46 (d, $J = 6.3$ Hz, 3H, CH_3CH), 2.47 (s, 3H, OCH_3), 3.64 (s, 1H, OH), 4.52 (q, $J = 6.3$ Hz, 1H, CH_3CH), 4.72 (d, $J = 1.6$ Hz, 1H, $\text{C}_C\text{HC}_C\text{COH}$), 5.55 (d, $J = 6.8$ Hz, 1H, $\text{C}_C\text{C}(t\text{-Bu})\text{C}_C\text{HC}_C\text{H}$), 5.60 (dd, $J = 6.8, 1.6$ Hz, 1H, $\text{C}_C\text{C}(t\text{-Bu})\text{C}_C\text{HC}_C\text{H}$), 7.32–7.41 (m, 10H, H_{ar}). ^{13}C NMR (90 MHz, CDCl_3): δ 22.0 (CH_3CH), 30.8 ($(\text{CH}_3)_3\text{C}$), 33.7 ($(\text{CH}_3)_3\text{C}$), 56.0 (OCH_3), 74.1 (CH_3CH), 81.5 (COH), 91.5 (C_CH), 92.1 (C_CH), 94.9 (C_CH), 117.6 (C_C), 117.7 (C_C), 121.1 (C_C), 127.5 (2C, $\text{C}_{\text{ar}}\text{H}$), 127.6 (2C, $\text{C}_{\text{ar}}\text{H}$), 127.8 ($\text{C}_{\text{ar}}\text{H}$), 128.1 (2C, $\text{C}_{\text{ar}}\text{H}$), 128.2

(38) Brock, C. P.; Duncan, L. L. *Chem. Mater.* **1994**, *6*, 1307–1312.

(2C, C_{ar}H), 128.5 (C_{ar}H), 144.2 (C_{ar}), 144.4 (C_{ar}), 233.6 (C≡O). MS (EI): *m/z* (%) 510 (M⁺, 18), 426 (M⁺ - 3CO, 100), 394 (M⁺ - 3CO - CH₃OH, 62), 350 (27), 311 (37), 269 (50), 255 (53). Anal. Calcd for C₂₉H₃₀CrO₅ (510.55): C, 68.22; H, 5.92. Found: C, 68.21; H, 5.95.

(-)-(1*P*R,1'*R*)-η⁶-[2-(1-Methoxyethyl)-5-*tert*-butyl-(diphenylhydroxymethyl)benzene]tricarbonylchromium(0), (-)-**3**. The procedure for the synthesis of the racemic complex (±)-**3** was followed.

Methylolithium (0.37 mL of a 1.49 M solution in diethyl ether, 0.55 mmol) was added dropwise at -78 °C to a stirred solution of tetramethylpiperidine (93 μL, 0.55 mmol) in THF (5 mL). Complex (-)-**2** (150 mg, 0.46 mmol) in THF (2 mL) was added followed by the addition of benzophenone (255 mg, 1.4 mmol) in THF (5 mL). Flash column chromatography gave (-)-**3** as a yellow solid (171 mg, 73%). mp: 173–178 °C. Enantiomeric excess was determined by HPLC analysis (Chiralcel ODH, 0.2% *i*-PrOH/*n*-hexane, 0.4 mL/min, 330 nm); (*R*) enantiomer *t_r* = 35.6 min (major); (*S*) enantiomer *t_r* = 40.9 min (minor): >93% ee. [α]_D²⁵ = -42.4° (*c* 0.75, CH₂Cl₂). All other data were identical to those obtained for (±)-**3**.

(±)-2-(1-Methoxyethyl)-5-*tert*-butyl-(diphenylhydroxymethyl)benzene, (±)-**4**. A solution of complex (±)-**3** (460 mg, 0.9 mmol) in diethyl ether (180 mL) was irradiated with a 100 W light bulb with slow stirring for 7 d. The resulting suspension was filtered through a pad of Celite, and the filtrate was evaporated under reduced pressure. Flash column chromatography of the residue (SiO₂; hexane/diethyl ether/NEt₃, 90:9:1) gave compound (±)-**4** as a white solid (243 mg, 72%). mp: 124–125 °C. IR (Nujol, cm⁻¹): ν_{OH} 3401 (s). IR (KBr, cm⁻¹): ν_{OH} 3444 (s), ν_{CH} 2965 (s), ν_{CH} 1446 (m), ν_{COC} 1096 (m), ν_{COC} 1068 (s), ν_{ar-CH} 841 (m), ν_{ar-CH} 763 (w), ν_{ar-CH} 751 (m), ν_{ar-CH} 700 (s). ¹H NMR (400 MHz, CDCl₃): δ 1.11 (s, 9H, (CH₃)₃C), 1.33 (d, *J* = 6.3 Hz, 3H, CH₃CH), 2.79 (s, 3H, OCH₃), 4.19 (s, 1H, OH), 4.64 (q, *J* = 6.3 Hz, 1H, CH₃CH), 6.66 (d, *J* = 2.1 Hz, 1H, C_{ar}HC_{ar}COH), 7.23–7.24 (m, 11H, H_{ar}), 7.46 (d, *J* = 8.1 Hz, 1H, H_{ar}). ¹³C NMR (100 MHz, CDCl₃): δ 21.3 (CH₃CH), 31.0 ((CH₃)₃C), 34.4 ((CH₃)₃C), 55.1 (OCH₃), 75.2 (CH₃CH), 83.1 (COH), 124.5 (C_{ar}H), 127.0 (C_{ar}H), 127.3 (C_{ar}H), 127.5 (2C, C_{ar}H), 127.7 (2C, C_{ar}H), 127.8 (2C, C_{ar}H), 127.88 (2C, C_{ar}H), 127.92 (2C, C_{ar}H), 139.5 (C_{ar}), 144.5 (C_{ar}), 146.7 (C_{ar}), 147.9 (C_{ar}), 149.0 (C_{ar}). MS (EI): *m/z* (%) 356 (M⁺ - H₂O, 100), 341 (M⁺ - H₂O - CH₃, 32), 324 (M⁺ - H₂O - CH₃OH, 52), 281 (M⁺ - H₂O - CH₃OH - C₂H₃O, 20), 265 (M⁺ - H₂O - C₇H₇, 72). Anal. Calcd for C₂₆H₃₀O₂ (374.52): C, 83.38; H, 8.07. Found: C, 83.47; H, 8.04.

(±)-(1*P*S,1'*S*,1'*R*)(1*P*R,1'*R*)-η⁶-[2-(1-Methoxyethyl)-5-*tert*-butyl-(1-η⁶-phenyl-tricarbonylchromium(0)-1-phenyl-1-hydroxymethyl)benzene]tricarbonylchromium(0), (±)-**5a**, and (±)-(1*P*R,1'*R*)-η⁶-[2-(1-Methoxyethyl)-5-*tert*-butyl-(1-η⁶-phenyl-tricarbonylchromium(0)-1-phenyl-1-hydroxymethyl)benzene]tricarbonylchromium(0), (±)-**5b**. A 25 mL round-bottomed flask fitted with a Liebig air condenser with a water condenser on top was charged with hexacarbonylchromium(0) (95 mg, 0.43 mmol), ligand (±)-**4** (162 mg, 0.43 mmol), dry THF (0.8 mL), and dry di-*n*-butyl ether (8 mL). The suspension was thoroughly saturated with nitrogen, before being heated to 130 °C, and refluxed under a slight nitrogen overpressure (40 mbar). After 48 h, the orange reaction mixture was allowed to cool to room temperature, and the solvent was removed in vacuo. Flash column chromatography (SiO₂; hexane/diethyl ether, 9:1) of the residue offered first the dichromium complex (±)-**5a** as a yellow solid (18 mg, 6%). mp: 161–164 °C (decomp). IR (Nujol, cm⁻¹): ν_{OH} 3544 (w), ν_{CO} 1972 (s), 1955 (sh), 1904 (m), 1887 (s), 1867 (sh). ¹H NMR (400 MHz, CDCl₃): δ 0.68 (d, *J* = 6.2 Hz, 3H, CH₃CH), 1.18 (s, 9H, (CH₃)₃C), 3.34 (s, 3H, OCH₃), 4.09 (s, 1H, OH), 4.58 (q, *J* = 6.2 Hz, 1H, CH₃CH), 4.89 (d, *J* = 6.4 Hz, 1H, *o*-C_{Cr}H), 4.98 (dt, *J* = 6.4, 1.0 Hz, 1H, *m*-C_{Cr}H), 5.17 (d, *J* = 1.6 Hz, 1H, C_{Cr}(*t*-Bu)C_{Cr}HC_{Cr}COH), 5.30 (d, *J* = 6.8 Hz, 1H, C_{Cr}(*t*-Bu)C_{Cr}HC_{Cr}H), 5.33 (dt, *J* = 6.4, 1.0 Hz, 1H, *m'*-C_{Cr}H), 5.59 (t, *J* = 6.4 Hz, 1H, *p*-C_{Cr}H), 5.69 (dd, *J* = 6.8, 1.6 Hz, 1H, C_{Cr}(*t*-Bu)C_{Cr}HC_{Cr}H), 6.37 (d, *J* = 6.4 Hz, 1H, *o'*-C_{Cr}H), 7.28–7.41 (m, 5H, H_{ar}). ¹³C NMR (100 MHz, CDCl₃): δ 20.1 (CH₃-

CH), 31.0 ((CH₃)₃C), 33.7 ((CH₃)₃C), 57.1 (OCH₃), 73.3 (CH₃CH), 79.0 (COH), 87.1 (C_{Cr}H), 87.9 (C_{Cr}H), 88.2 (C_{Cr}H), 93.1 (C_{Cr}H), 94.7 (C_{Cr}H), 95.2 (C_{Cr}H), 95.9 (C_{Cr}H), 96.0 (C_{Cr}H), 114.5 (C_{Cr}), 115.9 (C_{Cr}), 117.1 (C_{Cr}), 118.5 (C_{Cr}), 127.2 (2C, C_{ar}H), 128.2 (C_{ar}H), 128.5 (2C, C_{ar}H), 142.1 (C_{ar}), 231.8 (C≡O), 232.8 (C≡O). MS (FAB): *m/z* (%) 669 (M⁺ + Na, 7), 646 (M⁺, 4), 562 (M⁺ - 3CO, 77), 478 (M⁺ - 6CO, 33), 426 (M⁺ - 3CO - Cr(CO)₃, 100). Anal. Calcd for C₃₂H₃₀Cr₂O₈ (646.57): C, 59.44; H, 4.68. Found: C, 59.59; H, 4.57.

This was followed by complex (±)-**5b** as a yellow solid (13 mg, 5%). mp: 160 °C (decomp). IR (Nujol, cm⁻¹): ν_{OH} 3580 (w), ν_{CO} 1968 (s), 1960 (s), 1918 (m), 1879 (s), 1860 (s). ¹H NMR (400 MHz, CDCl₃): δ 1.18 (s, 9H, (CH₃)₃C), 1.37 (d, *J* = 6.3 Hz, 3H, CH₃CH), 2.45 (s, 3H, OCH₃), 3.71 (s, 1H, OH), 4.38 (q, *J* = 6.3 Hz, 1H, CH₃CH), 4.82 (d, *J* = 6.5 Hz, 1H, *o*-C_{Cr}H), 5.00 (dt, *J* = 6.5, 1.1 Hz, 1H, *m*-C_{Cr}H), 5.06 (d, *J* = 1.6 Hz, 1H, C_{Cr}(*t*-Bu)C_{Cr}HC_{Cr}COH), 5.34 (dt, *J* = 6.5, 1.1 Hz, 1H, *m'*-C_{Cr}H), 5.46 (d, *J* = 6.8 Hz, 1H, C_{Cr}(*t*-Bu)C_{Cr}HC_{Cr}H), 5.60 (t, *J* = 6.5 Hz, 1H, *p*-C_{Cr}H), 5.64 (dd, *J* = 6.8, 1.6 Hz, 1H, C_{Cr}(*t*-Bu)C_{Cr}HC_{Cr}H), 6.31 (d, *J* = 6.5 Hz, 1H, *o'*-C_{Cr}H), 7.40 (br s, 5H, H_{ar}). ¹³C NMR (100 MHz, CDCl₃): δ 22.1 (CH₃), 30.9 ((CH₃)₃C), 33.8 ((CH₃)₃C), 55.8 (OCH₃), 74.5 (CH₃CH), 79.3 (COH), 87.3 (C_{Cr}H), 88.5 (C_{Cr}H), 90.8 (C_{Cr}H), 92.3 (C_{Cr}H), 93.9 (C_{Cr}H), 94.2 (C_{Cr}H), 96.0 (C_{Cr}H), 96.1 (C_{Cr}H), 115.3 (C_{Cr}), 115.7 (C_{Cr}), 117.5 (C_{Cr}), 120.1 (C_{Cr}), 127.3 (2C, C_{ar}H), 128.2 (C_{ar}H), 128.6 (2C, C_{ar}H), 141.5 (C_{ar}), 231.8 (C≡O), 233.0 (C≡O). MS (FAB): *m/z* (%) 669 (M⁺ + Na, 87), 562 (M⁺ - 3CO, 100), 533 (M⁺ - 3CO - CHO, 53), 478 (M⁺ - 6CO, 87), 446 (M⁺ - 6CO - CH₃OH, 53), 426 (M⁺ - 3CO - Cr(CO)₃, 80). Anal. Calcd for C₃₂H₃₀Cr₂O₈ (646.57): C, 59.44; H, 4.68. Found: C, 59.52; H, 4.78.

Crystallography. Crystal data and data collection parameters are summarized in Table 1. Crystals were mounted on a thin glass fiber using silicon grease and cooled on the diffractometer to 100 K using an Oxford Cryostream low-temperature attachment. Oscillation frames each of width 1–2° in either ϕ or ω and of 10–60 s deg⁻¹ exposure time were recorded using a Nonius KappaCCD diffractometer, with a detector to crystal distance of 30 mm. Crystals were indexed from five preliminary frames each of 2° width in ϕ using the Nonius Collect package.³⁹ Final unit cell dimensions and positional data were refined on the entire data set along with diffractometer constants to give the final unit cell parameters. Integration and scaling (DENZO-SMN, Scalepack⁴⁰) resulted in data set corrected for Lorentz and polarization effects and for the effects of crystal decay and absorption by a combination of averaging of equivalent reflections and an overall volume and scaling correction. Structures were solved by direct methods (SHELXS-97⁴¹) and developed via alternating least squares cycles and difference Fourier synthesis (SHELXL-97⁴²) with the aid of the XSeed interface.⁴³ All non-hydrogen atoms were modeled anisotropically. Hydrogen atoms were placed in calculated positions and allowed to ride on the atoms to which they were attached with an isotropic thermal parameter 1.2 times that of the parent atom (1.5 times for CH₃ groups). Hydroxyl protons were located experimentally and treated likewise if refinement proved unfeasible. Hydrogen atom thermal parameters were fixed at 1.2 times those of the parent atom. All calculations were carried out either on a Silicon Graphics Indy workstation or an IBM-PC compatible personal computer. Atomic coordinates, bond lengths and angles, and thermal parameters have been deposited at the Cambridge Crystallographic Data Centre. See Information for Authors, Issue No. 1.

(39) Hoofst, R. *Collect*; Nonius: Delft, 1998.

(40) Otwinowski, Z.; Minor, W. In *Methods in Enzymology*; Carter, C. W., Sweet, R. M., Eds.; Academic Press: London, 1997; Vol. 276, pp 307–326.

(41) Sheldrick, G. M. *SHELXS-97*; University of Göttingen, 1997.

(42) Sheldrick, G. M. *SHELXL-97*; University of Göttingen, 1997.

(43) Barbour, L. J. *XSeed*; University of Missouri, Columbia, 1999.

(44) Janiak, C. *J. Chem. Soc., Dalton Trans.* **2000**, 3885–3896.

(45) Hunter, C. A.; Sanders, J. K. M. *J. Am. Chem. Soc.* **1990**, *112*, 5525–5534.

(46) Hunter, R.; Hauelsen, R. H.; Irving, A. *Angew. Chem., Int. Ed. Engl.* **1994**, *33*, 566–568.

Acknowledgment. We thank the EPSRC and King's College London for funding of the diffractometer system. Grateful acknowledgment is also given to the Nuffield Foundation for the provision of computing equipment.

Supporting Information Available: X-ray crystallographic file (CIF). This material is available free of charge via the Internet at <http://pubs.acs.org>.
JA012141M